Electron Diffraction of Optically Active Polyesters

Anna M. Ritcey, Josée Brisson, and Robert E. Prud'homme*

Département de Chimie, Centre de Recherche en Sciences et Ingénierie de Macromolécules, Université Laval, Sainte-Foy, Québec, Canada G1K 7P4

Received September 18, 1991; Revised Manuscript Received February 3, 1992

ABSTRACT: Crystal lattices for various polymorphs of poly(α-methyl-α-ethyl-β-propiolactone) (PMEPL) and poly(α-methyl-α-*n*-propyl-β-propiolactone) (PMPPL) are proposed on the basis of combined electron and X-ray diffraction data. Single-crystal-like electron diffraction is observed from melt-crystallized thin films of isotactic PMPPL, isotactic PMEPL, and the stereocomplex formed in mixtures of the two isotactic PMEPLs of opposite absolute configuration. Melt-crystallized isotactic PMEPL exhibits a monoclinic, pseudoorthorhombic lattice with the unit cell parameter *c* (4.75 Å) equivalent to the periodicity of the planar zigzag conformation typically obtained by sample elongation. The stereocomplex crystallizes in a distinctly different orthorhombic lattice with *c* = 7.1 Å, implying a 2_1 helical conformation. A third polymorph of PMEPL is found for atactic samples and solution-cast isotactic films. X-ray diffraction data for this form can be fitted satisfactorily with a unit cell analogous to the γ-phase previously reported for PPL, giving a value of *c* indicative of the helical conformation. Isotactic PMPPL crystallizes in an orthorhombic unit cell with *a* = 10.6 Å, *b* = 11.1 Å, and *c* = 6.7 Å.

Introduction

Polyesters belonging to the general class of α-disubstituted poly(β-propiolactones) are typically found to be semicrystalline and moreover, in some cases, exhibit polymorphism. The best characterized representative of this group is poly(α,α-dimethyl-β-propiolactone), known as poly(pivalolactone) (PPL), for which three crystal modifications[1-3] have been identified. In general, unoriented films crystallize as either the α- or γ-polymorph, with the formation of the latter favored by rapid quenching from the melt.[3] A transition to the β-form is induced by stretching,[1,4] and, consequently, X-ray diffraction fiber patterns of the α- or γ-form are difficult to obtain. Recently, however, the crystal structures of these two polymorphs of PPL have been determined from single-crystal-like electron diffraction. The α-phase is monoclinic (*a* = 9.03 Å, *b* = 11.62 Å, *c* = 6.01 Å, and γ = 121.5°) with each unit cell containing two antiparallel 2_1 helices of *opposite chirality*.[5] The γ-phase, on the other hand, is found to be orthorhombic (*a* = 8.23 Å, *b* = 11.28 Å, and *c* = 6.02 Å) and composed of antiparallel 2_1 helices of the *same chirality*.[6] Although the crystal structure of the β-phase of PPL has not been resolved, the fiber repeat distance of 4.76 Å measured by X-ray diffraction indicates that the polymer chains adopt a planar zigzag conformation in this polymorph.[4]

The X-ray fiber diagram of the α-modification of atactic poly(α-methyl-α-*n*-propyl-β-propiolactone) (PMPPL) has been obtained from stretched films of PMPPL–polyisobutylene graft copolymers.[7] The observed reflections can be indexed according to an orthorhombic unit cell containing four chains with *a* = 17.9 Å, *b* = 13.5 Å, and *c* = 12.0 Å. It is interesting to note that this unit cell resembles that determined by electron diffraction for the γ-phase of PPL, with the parameters *a* and *c* being doubled for PMPPL.

The β-forms of PMPPL[8] and PMEPL[9] present very similar X-ray fiber patterns, indexed in the case of PMPPL as an orthorhombic lattice with unit cell parameters *a* = 7.48 Å, *b* = 10.2 Å, and *c* = 4.7 Å. The periodicity along the chain direction is the same as that found for the β-form of PPL and is characteristic of the extended-chain conformation.

Additional variations in crystal structure are found for poly(β-propiolactones) in which the two α-substituents are not identical. In such cases, optically active polymers can be prepared[10,11] and the crystalline properties are found to depend, to varying degrees, on tacticity. Racemic and optically active PMPPL share the same X-ray diffraction pattern, although the melting temperature and enthalpy of fusion are found to increase with optical purity.[12] In contrast, significant differences in crystal structure between isotactic and atactic poly(α-phenyl-α-ethyl-β-propiolactone) have been demonstrated by X-ray diffraction.[11] PMEPL presents a more complex polymorphic behavior. The isotactic polymer exhibits two distinct crystal modifications, one favored by melt crystallization and the other by solution casting.[13] Solid-state NMR spectra indicate that these two polymorphs differ in polymer conformation and are therefore not analogous to the α- and γ-forms of PPL, which differ only in crystal packing. Melt-crystallized isotactic PMEPL is concluded to adopt an extended-chain conformation typically found for the β-form, whereas solution-cast samples adopt a helical conformation.

PMEPL also shows the phenomenon of stereocomplexation.[14] Equimolar mixtures of the two isotactic polymers of opposite absolute configuration crystallize with a morphology and crystal structure that are distinctly different from those of the individual isotactic components. In nonequimolar blends, stereocomplex formation occurs preferentially over the crystallization of the isotactic polymers and controls the morphology over a wide concentration range. Perhaps most striking is the observation that the stereocomplex melts 40 °C above the melting temperature of the individual isotactic components.

Stereocomplex formation and the variation of crystal structure with changes in tacticity illustrate the importance of stereoregularity in the determination of crystalline intermolecular interactions. In the case of PMEPL, the elevated melting temperature of the stereocomplex indicates the presence of favorable contacts between isotactic polymers of opposite absolute configuration that are not possible in the individual isotactic components. The identification of these interactions requires the determination of the crystal structures of the various polymorphs, and, for this reason, the present electron and X-ray diffraction study has been undertaken.

0024-9297/92/2225-2705$03.00/0

Experimental Section

PMEPL of varying degrees of optical purity were prepared and characterized by Grenier et al.[10] PMPPL samples were synthesized by Ambeault.[15]

Samples for electron microscopy were cast directly on carbon-coated microscope grids (200 mesh) from single drops (4–6 μL) of 0.01% solutions in hexafluoroisopropyl alcohol. Melt crystallization was performed by heating the grids, either under vacuum or in a nitrogen atmosphere, to temperatures 20 °C above the melting point of the polymer and subsequently cooling them to room temperature at a cooling rate of 1 °C/min.

In the case of epitaxially crystallized samples, 1 drop of a saturated solution of anthracene in xylene was deposited on the grid-supported polymer films prior to melt crystallization. In addition, these grids were sealed in small glass tubes before heating to impede the sublimation of anthracene. After melt crystallization as described above, the grids were either washed in acetone vapor or heated at 50 °C under vacuum to remove the anthracene.

All samples for X-ray diffraction were initially prepared as films cast at room temperature from solution in hexafluoroisopropyl alcohol, the only known good solvent for isotactic PMEPL. Melt-crystallized samples were obtained by the subsequent heating of these films, under vacuum, to temperatures 20 °C above the melting point, followed by cooling at 1–3 °C/min. Films of the stereocomplex were prepared by casting from solutions containing equal concentrations of the two isotactic polymers of opposite absolute configuration.

Isotactic PMEPL was also crystallized from dilute solution in diethyl carbonate, propylene carbonate, *n*-butanol, and amyl acetate. For all solvents, solutions containing 0.05% polymer were prepared by heating at 140 °C. The solutions were rapidly cooled to crystallization temperatures ranging from 75 to 100 °C. After 2–5 days, the crystalline precipitate was isolated by filtration.

Electron diffraction patterns were observed with a Phillips EM 420 electron microscope, operated at 100–120 kV, and recorded with Kodak electron image film SO-163. Gold, deposited on representative samples, served as a standard for the calibration of measured *d*-spacings. For each polymer, samples of various thicknesses were examined for differences in relative intensities or systematic absences.

X-ray diffraction powder patterns were recorded with a Rigaku Model RU200B rotating-anode generator at 55 kV and 190 mA, using Cu Kα, Ni-filtered radiation. The θ–2θ transmission geometry was used for all samples. Since X-ray spectra appear in a previous publication,[13] only the *d*-spacings and relative intensities are presented here.

Results and Discussion

Thin polymer films, crystallized directly on microscope grids as outlined above, exhibit no well-defined morphology when examined by transmission electron microscopy but appear as featureless dark patches under the electron beam. Distinct single-crystal-like diffraction patterns are, nevertheless, obtained for various samples and are reported in Figures 1–6. Within a given sample, the intensity of electron diffraction is found to vary greatly from one region to another, indicating nonuniformity in film thickness. In all cases, however, the relative intensity of the various diffraction spots, as well as the observation of systematic absences, is independent of sample thickness, suggesting that significant double diffraction does not occur.

Isotactic Poly(α-methyl-α-ethylpropiolactone) (PMEPL). Thin films of isotactic PMEPL prepared by direct melt crystallization on a microscope grid show the single-crystal-like electron diffraction pattern illustrated in Figure 1. If it is assumed that this diffraction pattern, obtained with irradiation normal to the sample surface, is the *hk*0 reciprocal lattice, the unit cell parameters *a* and *b* can be explicitly evaluated as 9.10 and 7.44 Å, respectively, with $\gamma = 90°$. Unfortunately no higher order reflections were recorded from tilted samples, presumably because of the weak intensity of the *hkl* reflections accessible through such experiments. The periodicity along the c direction was therefore evaluated from epitaxially crystallized samples.

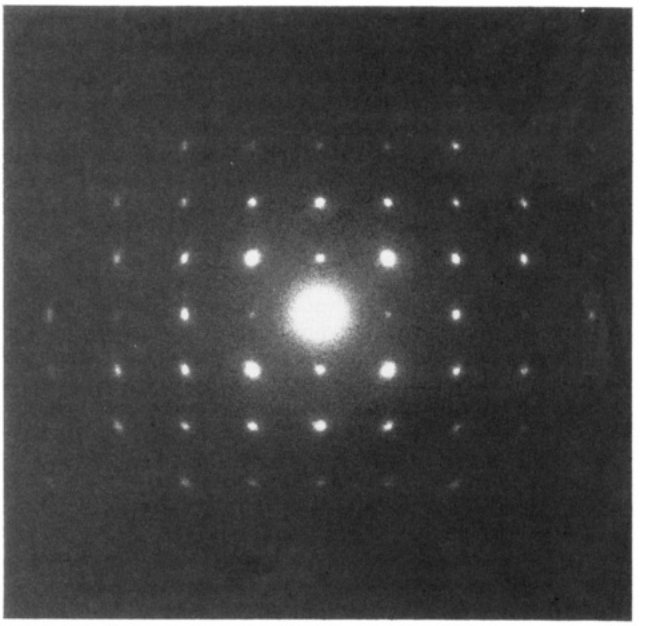

Figure 1. Electron diffraction pattern observed for melt-crystallized isotactic PMEPL with irradiation normal to the sample surface, identified as the *hk*0 reciprocal lattice (a*, vertical; b*, horizontal).

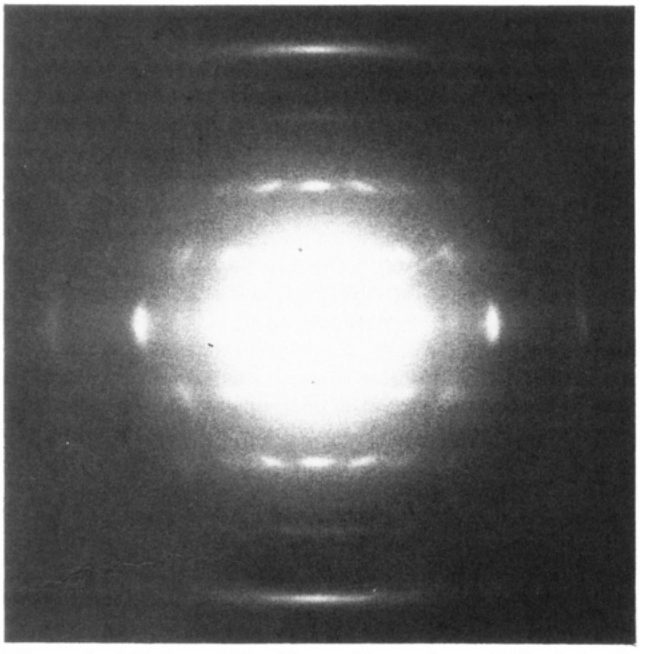

Figure 2. Electron diffraction pattern observed for isotactic PMEPL crystallized in the presence of anthracene, identified as the 0*kl* reciprocal lattice (c*, vertical; b*, horizontal).

Films of PMEPL crystallized in the presence of anthracene give rise to the diffraction pattern shown in Figure 2, which is distinctly different from that of Figure 1. The two characteristic periodicities of this reciprocal lattice correspond to crystal spacings of 7.35 and 4.75 Å. The former spacing agrees well with the value of *b* obtained above and Figure 2 can therefore be identified as the 0*kl* reciprocal lattice with $c = 4.75$ Å and $\alpha = 90°$. Both diffraction patterns exhibit a 2*mm* symmetry, consistent with an orthorhombic space group, and together yield an

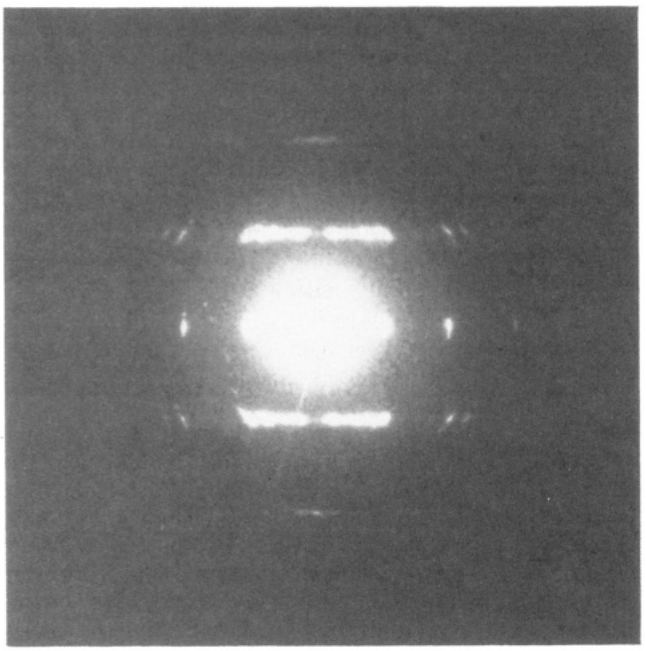

Figure 3. Electron diffraction pattern observed for the PMEPL stereocomplex with irradiation normal to the sample surface, identified as the $hk0$ reciprocal lattice (a*, vertical; b*, horizontal).

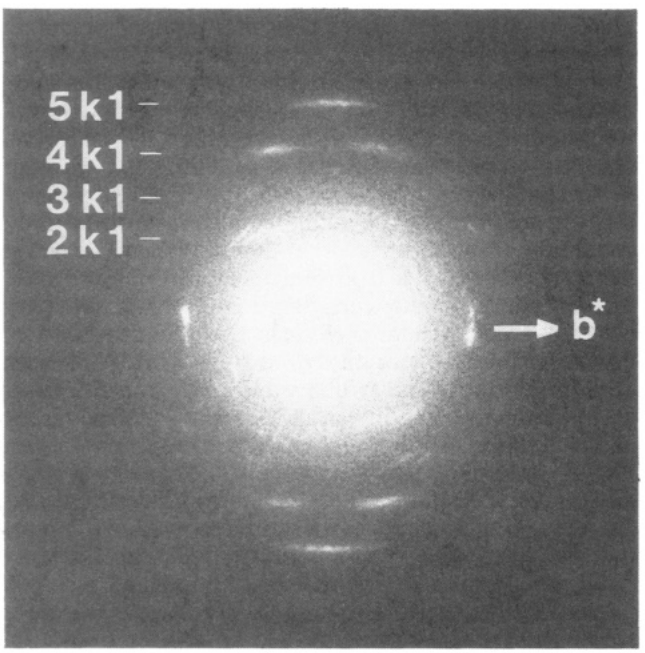

Figure 4. Electron diffraction pattern observed for the PMEPL stereocomplex with the sample tilted by 30° about b*.

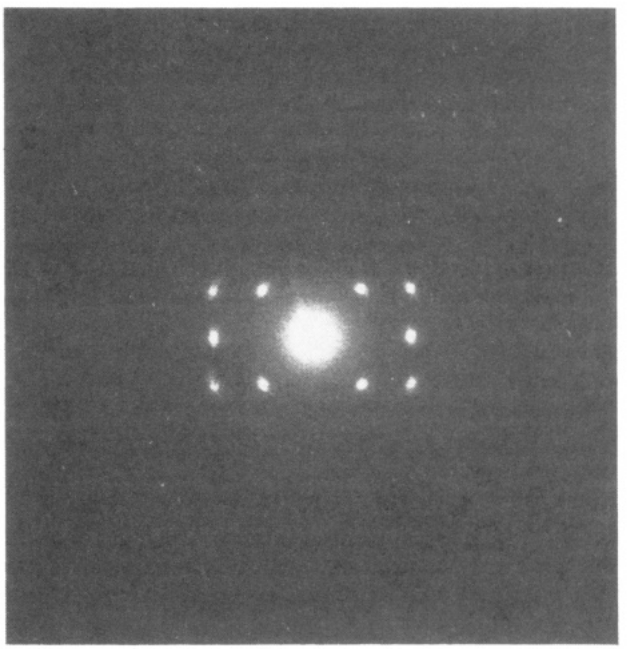

Figure 5. Electron diffraction pattern observed for melt-crystallized isotactic PMPPL with irradiation normal to the sample surface, identified as the $hk0$ reciprocal lattice (a*, horizontal; b*, vertical).

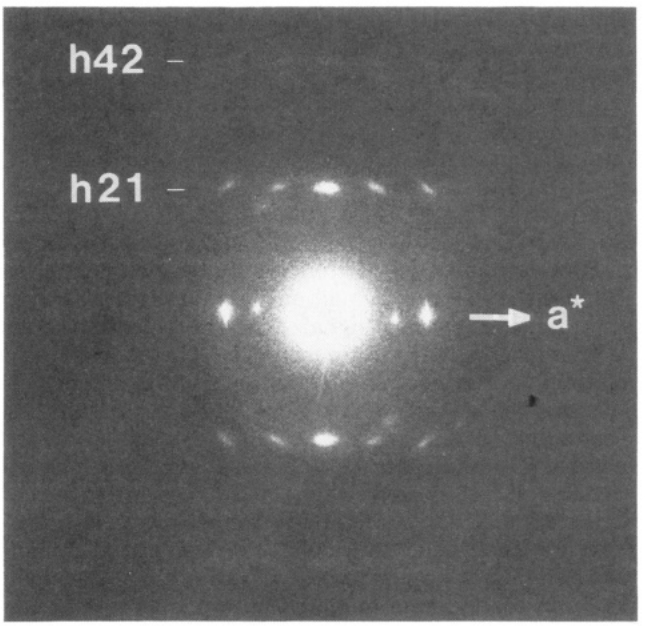

Figure 6. Electron diffraction pattern observed for isotactic PMPPL with the sample tilted by 40° about a*.

orthorhombic lattice with unit cell dimensions a = 9.10 Å, b = 7.44 Å, and c = 4.75 Å.

Epitaxial crystallization of aliphatic polyesters on anthracene has been previously reported.[16] Poly(hexamethylene oxalate) and poly(decamethylene oxalate) were both found to crystallize with the b axis perpendicular to the (001) face of anthracene crystals and the chain axis along the ⟨110⟩ direction. In this orientation, the two substrate periodicities[17] relevant to the consideration of lattice matching are the intermolecular distance of 5.24 Å along ⟨110⟩ and the 110 inter-row spacing of 4.93 Å. These distances (or multiples thereof) differ from the polyoxylate unit cell parameters a and c by 8–14%. In the present case, the orientation of PMEPL crystallites relative to the substrate is unknown. (In order to avoid vaporization in the vacuum of the electron microscope, the anthracene was removed prior to the electron diffraction measurements and hence no patterns showing simultaneous diffraction from the polymer and substrate were observed.) The close agreement between the polymer chain repeat distance (4.75 Å) and the 110 inter-row spacing of anthracene (4.93 Å) suggests, however, that PMEPL may crystallize perpendicular to the ⟨110⟩ direction of anthracene. If this is so, the lattice matching between the b direction of the polymer crystals and the intermolecular distance of the substrate is rather poor (7.35 Å versus 5.24 Å).

X-ray diffraction data for melt-crystallized isotactic PMEPL can be fitted with the orthorhombic unit cell determined by electron diffraction, as summarized in Table I. Moreover, the strongest reflections in the electron diffraction pattern of Figure 1, indexed as 110, 200, 020,

Table I
X-ray Diffraction Data for Isotactic PMEPL Prepared by Melt Crystallization[a]

d_{obs}/Å (I_{rel})	hkl	d_{calc}/Å
9.09 (37)	100	9.10
5.79 (100)	110	5.76
4.55 (19)	200	4.55
4.00 (12)	011	4.00
3.90 (16)	210	3.88
3.77 (13)	020	3.72
3.49 (19)	120	3.44
3.25 (6)	201	3.29
2.91 (8)	021, 220	2.93
2.43 (8)	311, 130	2.42, 2.40
2.36 (6)	002, 320	2.38, 2.35
2.28 (6)	102, 400, 012	2.30, 2.28, 2.26
2.16 (7)	230, 410	2.18

[a] Observed distances and relative intensities are given in column 1. The calculated d-spacings of column 3 correspond to an orthorhombic unit cell with a = 9.10 Å, b = 7.44 Å, and c = 4.75 Å.

100, 120, and 130, appear as intense peaks in the X-ray spectrum. This indicates that the electron diffraction pattern of Figure 1 is indeed representative of the bulk melt-crystallized sample from which the powder X-ray pattern was recorded. Very few higher order reflections appear on the X-ray diagram, which accounts for the fact that no higher order reflections were observed by electron diffraction tilt experiments. In order to record the most intense hkl reflection, 011, it would be necessary to tilt the sample by 57°, an angle outside of the range of experimentally accessible values. All other hkl reflections are very weak.

A similar comparison of X-ray and electron diffraction data is more limited in the case of the epitaxially crystallized sample: the only reflections observed by X-ray diffraction which are expected to appear in the $0kl$ reciprocal lattice are those indexed as 011 and 020. The latter is evident in the electron diffraction pattern of Figure 2. However, since the 011 reflection would appear in the region of the electron diffraction diagram that is obscured by the large background signal of the direct electron beam, its presence cannot be ascertained. The most intense reflection of the electron diffraction diagram, indexed as 040, is not observed in the X-ray data because of the corresponding small d-spacing (1.86 Å). Nevertheless, the fact that all of the X-ray data can be satisfactorily indexed with c = 4.75 Å suggests that the diffraction pattern of Figure 2 is indeed characteristic of melt-crystallized isotactic PMEPL and not a unique form induced by epitaxial effects. The periodicity of 4.75 Å along the chain direction corresponds to that of the planar zigzag conformation, and the diffraction results thus agree with the conclusion of a recent solid-state NMR study,[13] namely, that isotactic PMEPL crystallizes from the melt as an extended chain.

From electron diffraction, it is proposed that no systematic absences appear on $hk0$, $0kl$, $00l$, $h00$, and $0k0$. In the case of $hk0$, $0kl$, and $h00$, this hypothesis is confirmed by X-ray diffraction, where the 110, 011, and 100 reflections are clearly observed. Furthermore, the unambiguous observation of the 201 reflection in the X-ray diffraction data eliminates the possibility of systematic absences for $h0l$. The only orthorhombic space groups consistent with these observations are $P222$, $Pmm2$, $Pm2m$, $P2mm$, and $Pmmm$. In addition, since isotactic PMEPL is chiral, all space groups having mirror planes can be discounted, leaving only one possible orthorhombic space group, namely, $P222$.

Density measurements indicate that two repeat units of PMEPL are present in the orthorhombic unit cell. (For Z = 2, the calculated density of 1.18 g·cm^{-3} agrees satisfactorily with the experimental value of 1.10 g·cm^{-3}.) However, in the $P222$ space group, the general position has a multiplicity of 4, and it should therefore be concluded that the polymer chain occupies a special equipoint. The only possibility in the $P222$ space group, a 2-fold symmetry axis, is incompatible with the chiral repeat unit of isotactic PMEPL which cannot accommodate any symmetry element. The same difficulty would be encountered with any orthorhombic space group, since the minimum multiplicity for the general position is 4.

It is, however, possible to find a monoclinic space group consistent with the experimental data. The only space group which agrees with the electron diffraction observations (again excluding space groups containing mirror planes) would then be $P2$, in which the general position accommodates two repeat units. In this space group, the chains could be packed parallel or antiparallel, depending on the identity of the unique axis. The determination of the unique axis is straightforward: in this space group, the only zero level which does not present a $2mm$ symmetry is the one perpendicular to the unique axis. Since the two observed zero levels ($hk0$ and $0kl$) show a $2mm$ symmetry, the b axis is proposed to be the unique axis. The chains should therefore be packed antiparallel to one another, as expected to permit chain folding.

Despite the precautions taken to minimize multiple scattering, there is always a danger of missing systematic absences in electron diffraction because of this effect. In the present case, this possibility must be considered for absences on $00l$ and $0k0$. The conclusion that no systematic absences occur on these layer lines is based on the observation of reflections indexed as 001, 003, 010, and 030 in the electron diffraction diagram. Since corresponding reflections cannot be unambiguously identified in the X-ray diffraction spectrum, the possibility that the electron diffraction spots arise from multiple scattering cannot be discounted. Symmetry considerations prohibit systematic absences on $00l$ in a monoclinic lattice, and thus only the possibility of absences on $0k0$ must be considered. An absence along this layer line would lead to a $P2_1$ space group, indicating, as in the case of the $P2$ space group deduced above, antiparallel chain packing.

Since the observed angle β is very close to 90°, it is not possible to distinguish between $\bar{h}kl$ and hkl reflections using X-ray diffraction, and the X-ray data fit equally well for a monoclinic or an orthorhombic unit cell.

The existence of a pseudoorthorhombic unit cell in this particular form of PMEPL may well be the result of the pseudosymmetry of the chain in the all-trans conformation. In this conformation, the plane of the polymer chain is distinct from a mirror plane only by the presence of a supplementary carbon atom on one of the α-substituents.

It is interesting to note the similarity between the unit cell parameters obtained for melt-crystallized isotactic PMEPL and those reported for the β-form of PMPPL. One of the crystal dimensions is slightly larger in the case of PMPPL, as would be expected to accommodate the additional side-chain methylene group. This result, in conjunction with the observation that the X-ray diffraction diagrams of the β-forms of PMEPL[9] and PMPPL[8] are near identical, suggests that PMEPL crystallizes from the melt in the same crystal modification as is obtained upon elongation.

Samples of isotactic PMEPL crystallized at elevated temperatures from dilute solution in diethyl carbonate, propylene carbonate, n-butanol, or amyl acetate show the same X-ray diffraction pattern as melt-crystallized films.

Table II
X-ray Diffraction Data for the Stereocomplex Formed by Isotactic PMEPLs of Opposite Absolute Configuration[a]

d_{obs}/Å (I_{rel})	hkl	d_{calc}/Å
8.55 (100)	040	8.55
5.87 (56)	200, 210	5.90, 5.82
5.61 (52)	220	5.58
5.32 (55)	131, 230	5.36, 5.24
4.91 (35)	141, 051, 240	4.95, 4.92, 4.84
4.41 (30)	250, 221	4.47, 4.38
4.01 (27)	231, 241	4.01, 3.96
3.30 (22)	122, 331, 042	3.33, 3.29, 3.28
3.15 (15)	341, 142, 052	3.19, 3.16, 3.15
2.72 (13)	252, 401, 411	2.77, 2.72, 2.72
2.65 (6)	431, 302, 312	2.65, 2.63, 2.63
2.54 (9)	451	2.53
2.31 (12)		
2.22 (5)		
2.10 (11)		

[a] Observed distances and relative intensities are given in column 1. The calculated d-spacings of column 3 correspond to an orthorhombic unit cell with a = 11.8 Å, b = 34.2 Å, and c = 7.1 Å. Many possibilities exist for the indexation of the last three reflections.

Single crystals were never obtained, and no electron diffraction was observed from these samples.

Stereocomplex Formed by PMEPL. Thin films of PMEPL containing equal quantities of the two isotactic polymers of opposite absolute configuration give rise to the unique electron diffraction pattern shown in Figure 3. The striking contrast between this pattern and that obtained for the pure isotactic components (Figure 1) signifies that major differences in crystal structure exist between the stereocomplex and its individual isotactic components. If it is again assumed that this diffraction pattern is the $hk0$ reciprocal plane, the following unit cell parameters can be directly evaluated: a = 5.88 Å, b = 34.2 Å, and γ = 90°.

As illustrated in Figure 4, additional reflections are observed upon tilting of the sample by 30° about the b axis. Indexation of the first stratum, which has a d^* spacing of 0.22 Å^{-1}, is only possible with h = 1, yielding c = 7.1 Å. The strata at d^* = 0.30 Å^{-1} and d^* = 0.45 Å^{-1} cannot, however, be indexed with these unit cell parameters. The value of a was therefore doubled, allowing the indexation of all diffraction strata, as shown in Figure 4, with c = 7.1 Å. The doubling of a indicates the presence of a systematic absence for h = odd on the $hk0$ level. Unfortunately, no good photographs, which could have confirmed the doubling, were obtained from tilt experiments around the a axis, perhaps because the large value of b results in a close succession of layer lines that are difficult to distinguish.

The X-ray diffraction data summarized in Table II can be successfully indexed with the orthorhombic unit cell parameters determined by electron diffraction (a = 11.8 Å, b = 34.2 Å, and c = 7.1 Å). All major reflections observed in the electron diffraction patterns of Figures 3 and 4 are present in the X-ray diagram. The observed density of the stereocomplex, 1.02 g·cm^{-3}, is compatible with the value calculated for 16 repeat units per unit cell (1.06 g·cm^{-3}). This is a reasonable result since many orthorhombic space groups have general or special positions which can accommodate 16 motifs.

From electron diffraction, it is possible to identify the $hk0$ (h = 2n) and $0k0$ (k = 2n) systematic presences. It is, however, not possible to determine without ambiguity the other systematic absences that could be present, since, with the large unit cell of this sample, X-ray diffraction indexation is not unambiguous. Further work is therefore necessary to determine the space group of this crystal form.

Table III
X-ray Diffraction Data for the Isotactic PMPPL[a]

d_{obs}/Å (I_{rel})	assignment	d_{calc}/Å
7.67 (100)	110	7.67
5.28 (33)	200	5.30
4.78 (35)	210	4.78
4.26 (15)	021	4.28
3.92 (12)	211	3.90
3.50 (6)	130	3.49
3.34 (6)	310, 002, 221	3.37, 3.37, 3.33
3.08 (9)	131, 112, 230	3.10, 3.08, 3.09
2.74 (5)		
2.45 (5)		
2.22 (4)		

[a] Observed distances and relative intensities are given in column 1. The calculated d-spacings of column 3 correspond to an orthorhombic unit cell with a = 10.6 Å, b = 11.1 Å, and c = 6.7 Å. Many possibilities exist for the indexation of the last three reflections.

It is interesting to note that the periodicity along the chain axis (7.1 Å) is very close to that of a perfect $(t_2g_2)_2$ conformation with t = 180° and g = 60°. This represents the first example of a poly(β-propiolactone) for which the repeat distance of the ideal 2_1 helix has been observed. In most cases, the torsion angles are found to deviate from 180° and 60°, resulting in a shortening of the fiber repeat distance.[5,6] For example, PPL is characterized by a value of c = 6.0 Å in both the α- and γ-phase.[5,6] Various conformations with this repeat distance have been considered,[5,6,18,19] differing in the degree to which each of the four torsion angles departs from the ideal values. The possible deviation from planarity of the ester linkage has been of particular interest.[20] Conformational analysis of isolated chains[21] indicates that the perfect $(t_2g_2)_2$ conformation is energetically allowed, differing by only 1–2 kcal mol^{-1} from the various conformations proposed for a fiber repeat distance of 6.0 Å. It therefore appears probable that, in the case of the stereocomplex, the observed periodicity of 7.0 Å does indeed correspond to a 2_1 helix with torsion angles very close to their usual equilibrium values of ±60° and 180°. Although it is not clear why deviations from this conformation are observed in some cases and not in others, recent calculations[22] have demonstrated that the differences in torsion angles found for α- and γ-PPL can be accounted for by the consideration of packing energies. Resolution of the crystal structures of the various forms of PMEPL should yield interesting information in this regard.

Poly(α-methyl-α-*n*-propylpropiolactone) (PMPPL). A third distinct electron diffraction pattern is observed for isotactic PMPPL, as illustrated in Figure 5. From this diagram, the unit cell parameters a and b can be evaluated as 10.6 and 11.1 Å, respectively, with γ = 90°. Upon tilting of the sample by 40° about the a axis, two new series of diffraction spots are observed, which can be indexed as h21 and h42, giving c = 6.7 Å. As in the two previous cases, the X-ray data obtained from a bulk sample can be indexed to fit the same unit cell parameters as found by electron diffraction. The principal reflections of the diffraction pattern, namely, 110, 210, 200, and 021, all appear among the most intense X-ray reflections, as summarized in Table III. This unit cell contains four repeat units, as determined by the measured density of 1.10 g·cm^{-3}. The density calculated from the reported unit cell parameters is 1.08 g·cm^{-3}, and although this value is smaller than the observed one, the difference can be easily accounted for by the experimental error in the determination of c from the tilt experiments. A decrease in c of only 3% yields a calculated density greater than the measured 1.10 g·cm^{-3}.

Table IV
X-ray Diffraction Data for Atactic PMEPL[a]

	assigned from isotactic PMPPL		assigned from γ-phase PPL	
d_{obs}/Å	hkl	d_{calc}/Å	hkl	d_{calc}/Å
8.68	110	8.69	110	8.69
5.96	011	6.00	020	5.97
5.19	200	5.19	011	5.18
4.14	031	4.11	021	4.14
3.78	131	3.82	130	3.80
3.27	002	3.24	031	3.27
3.03	022	3.00	040	2.98
2.68	132	2.67	240	2.70
2.32	421	2.30	032	2.33
2.08	441	2.06	042	2.07

[a] Indexation by analogy to isotactic PMPPL and to the γ-phase of PPL is presented with corresponding calculated spacings. The unit cell parameters were evaluated, by the least-squares fitting of the observed d-spacings to an orthorhombic lattice, as a = 10.4 Å, b = 15.9 Å, and c = 6.5 Å and a = 12.6 Å, b = 11.9 Å, and c = 5.8 Å, respectively, with reliability indices, R, of 0.07 and 0.04.

Table V
X-ray Diffraction Data for Solution-Cast Isotactic PMEPL[a]

	assigned from stereocomplex		assigned from γ-phase PPL	
d_{obs}/Å	hkl	d_{calc}/Å	hkl	d_{calc}/Å
8.51	040	8.50	110	8.50
5.72	210	5.76	020	5.72
5.26	230	5.20	011	5.22
4.79	240	4.82	111	4.83
4.32	221	4.29	201	4.31
3.83	241	3.93	121	3.90
3.23	122	3.21	031	3.20
2.78	401	2.69	112	2.78
2.42	342	2.45	222	2.42
2.14	442	2.15	402	2.15

[a] Indexation by analogy to the stereocomplex of PMEPL and to the γ-phase of PPL is presented with corresponding calculated spacings. The unit cell parameters were evaluated, by the least-squares fitting of the observed d-spacings to an orthorhombic lattice, as a = 11.7 Å, b = 34.0 Å, and c = 6.8 Å and a = 12.7 Å, b = 11.4 Å, and c = 5.9 Å, respectively, with reliability indices, R, of 0.11 and 0.05.

From the electron diffraction diagram, the systematic absences $h00$ ($h \neq 2n$) and $0k0$ ($k \neq 2n$) can be identified. The indexation of the X-ray data agrees with this observation and indicates that no supplementary systematic absences are present on $0kl$ and $h0l$. The $00l$ reflections, as is often the case for most polymers, cannot be observed from the powder diagram, and systematic absences for this class of reflection cannot be ascertained. Two space groups can be proposed on the basis of these observations: the $P2_12_12$ and $P2_12_12_1$ space groups, which both lead to antiparallel packing of the chains and differ mainly by the relative elevation of the polymer chains along the c axis in the unit cell. For both space groups, the polymer chain occupies a general position in the unit cell.

It is interesting to note that the value for the c axis for PMPPL (6.7 Å) lies between that of helical PPL (6.02 Å) and that obtained for the PMEPL stereocomplex (7.1 Å). It can be proposed, on this basis, that the conformation of the main chain should be $(t_2g_2)_2$, with deviations from the ideal trans and gauche torsion angle values, but to a lesser extend than found for PPL.

The unit cell obtained here for isotactic PMPPL differs significantly from that deduced from X-ray fiber data for the α-phase of atactic PMPPL[7] and for optically active samples of low optical purity.[12] This difference is not due solely to changes in indexation (the X-ray reflections reported in Table III for isotactic PMPPL are not the same as those previously reported[12]) but to real differences in structure.

Other Forms of PMEPL. Films of atactic PMEPL prepared either by solution casting or melt crystallization do not show single-crystal-like electron diffraction. Attempts were made, however, to index the X-ray powder pattern of this polymer with the various crystalline forms known for the poly(propiolactones). Indexation by comparison to the X-ray reflection assignments deduced for either melt-crystallized isotactic PMEPL or the stereocomplex was found to be totally unsatisfactory. The observation that atactic PMEPL crystallizes in a form different from that found for the stereocomplex is in agreement with the previously reported statistical nature of the atactic polymer.[23] The presence of long runs of repeat units of a given absolute configuration would be expected to result in a crystal structure similar to that found for the mixture of the two isotactic polymers, which is clearly not the case.

As summarized in Table IV, a reasonable fit of the experimental data for atactic PMEPL is possible by analogy to either isotactic PMPPL or the γ-phase of PPL. Of the two possibilities, the indexation obtained by comparison to PPL is preferred for two reasons: First, all of the reflections observed for atactic PMEPL can be indexed as reflections which appear for the γ-phase of PPL. This is not the case for the assignments made by comparison to PMPPL where some reflections (i.e., 011 and 031) appear in the data for atactic PMEPL but not in that for PMPPL. The second reason for which the analogy to the γ-phase of PPL is favored is that it provides the more reasonable unit cell parameters. Comparison to PMPPL produces the unlikely result of a larger unit cell for PMEPL than PMPPL.

Similarly, although electron diffraction was not observed from solution-cast films of isotactic PMEPL, the X-ray powder data can be indexed by analogy to both the stereocomplex and the γ-phase of PPL, as summarized in Table V. Despite the larger unit cell of the stereocomplex, the best fit is found for the comparison with PPL. The unit cell parameters obtained with the indexation according to the γ-phase of PPL are in good agreement with those found for atactic PMEPL.

Crystalline Densities. A comparison of the crystalline densities calculated from the unit cell parameters reveals several results that warrant further discussion. For example, isotactic PMEPL crystallizes from the melt to give a crystal form which is denser than that obtained for the stereocomplex. This appears to be contrary to what would be predicted from the equilibrium melting temperatures of these two crystal modifications. In this case, however, the two crystal structures differ not only in molecular packing but also in polymer conformation. Isotactic PMEPL crystallizes from the melt as a planar zigzag, a conformation which facilitates dense packing of the polymer chains. The resulting crystal form is, however, destabilized relative to the stereocomplex because the extended-chain conformation is of higher energy than the preferred 2_1 helix.[18]

The crystalline density and unit cell parameters of melt-crystallized isotactic PMEPL should rather be compared with the values found for the β-phase of PMPPL, which is also composed of chains in the planar zigzag conformation. As shown in Table VI, the calculated densities of these two forms are essentially identical and the unit cells differ only in one lateral dimension. The larger unit cell is found for PMPPL, the polymer with the longer side chain.

Table VI
Summary of Equilibrium Melting Temperature, Calculated Density, and Orthorhombic Unit Cell Parameters for Various Forms of PMEPL[a]

	T_f°, °C	density, g/cm³	Z	a, Å	b, Å	c, Å
isotactic PMEPL melt crystallized	164[25]	1.18 ± 0.01	2	9.10 ± 0.02	7.44 ± 0.02	4.75 ± 0.02
isotactic PMEPL solution cast*		0.89 ± 0.04	4	12.7 ± 0.2	11.4 ± 0.2	5.9 ± 0.1
atactic PMEPL*	121[25]	0.88 ± 0.04	4	12.6 ± 0.2	11.9 ± 0.2	5.8 ± 0.1
PMEPL stereocomplex	202[26]	1.06 ± 0.06	16	11.8 ± 0.2	34.2 ± 0.2	7.1 ± 0.2
PPL γ-phase[6]		1.19	4	8.23	11.28	6.02

[a] For comparison literature values for the γ-phase of PPL are also shown. Unit cell parameters for samples marked with an asterisk were evaluated from X-ray diffraction data only, indexed according to the γ-phase of PPL.

Table VII
Summary of Equilibrium Melting Temperature, Calculated Density, and Orthorhombic Unit Cell Parameters for Various Forms of PMPPL

	T_f°, °C	density, g/cm³	Z	a, Å	b, Å	c, Å
PMPPL isotactic		1.08 ± 0.03	4	10.6 ± 0.1	11.1 ± 0.1	6.7 ± 0.1
PMPPL atactic α-phase[7]	97[12]	1.17	16	17.9	13.5	12.0
PMPPL atactic β-phase[8]		1.19	2	7.48	10.2	4.7

The crystalline density of the stereocomplex can be compared to that calculated for isotactic solution-cast PMEPL, since these forms are both composed of molecules in the helical conformation. The stereocomplex is found to have the higher density, in accordance with both its higher melting temperature and the generalization that dense packing is more easily achieved for helices of opposite handedness than for helices of a single chirality.

An anomaly in crystalline densities is also apparent for PMPPL. The density calculated for isotactic PMPPL (1.08 g/cm³) is found to be lower than that evaluated from previously reported unit cell parameters[7] for the α-phase of the atactic polymer (1.17 g/cm³). This difference may be due to experimental uncertainties associated with the unit cell parameters, which can be predicted to be more significant in the case of the atactic polymer for which only X-ray fiber diffraction data are available. The calculated crystalline density and unit cell parameters determined for isotactic PMPPL in the present study are consistent with the values obtained for the γ-form of PPL.[6]

A further irregularity is evident upon comparison of isotactic PMPPL and solution-cast isotactic PMEPL. The polymer with the longer side chain (PMPPL) has the higher calculated crystalline density. As mentioned above, these two polymers do not share a common crystal form and the X-ray diffraction data of solution-cast PMEPL cannot be indexed with the unit cell found for PMPPL. In addition, the periodicities along the chain direction (6.7 Å for PMPPL and 5.9 Å for solution-cast PMEPL) indicate that significant differences also exist in the helical conformations adopted by these polymers. The observation that isotactic PMPPL and isotactic PMEPL do not exhibit the same conformations or crystal modifications is rather unexpected and can be explained only through the eventual determination of the crystal structures involved.

Conclusions

Several crystalline forms of two disubstituted poly(β-propiolactones), PMEPL and PMPPL, have been investigated by combined electron and X-ray diffraction measurements. The proposed unit cell parameters of the various samples are summarized in Tables VI and VII.

Three polymorphs of PMEPL are identified. Melt-crystallized isotactic PMEPL crystallizes in a monoclinic, pseudoorthorhombic lattice. The unit cell parameters indicate that this form is equivalent to the previously reported β-modification obtained by sample elongation and consists of polymer molecules in the extended conformation. The same polymorph is found for isotactic PMEPL crystallized from dilute solution at elevated temperatures. The stereocomplex formed by equimolar mixtures of isotactic PMEPL of opposite absolute configuration crystallizes in an orthorhombic lattice, with a periodicity along the chain direction equivalent to that of an ideal 2_1 helix, without deviation of the ester linkage from planarity. The third polymorph of PMEPL is found for atactic samples and solution-cast isotactic films. X-ray diffraction data for these forms can be fitted satisfactorily with a unit cell analogous to the γ-phase of PPL, giving a value of c implying a helical conformation. No monoclinic phase corresponding to the α-phase of PPL was found for the samples examined.

Isotactic PMPPL also crystallizes in an orthorhombic unit cell, giving an electron diffraction pattern distinctly different from PMEPL. The periodicity along the c axis indicates a helical conformation with deviations from the ideal conformation intermediate between the undeformed stereocomplex and the previously reported PPL.

Several general conclusions can be drawn from the polymorphic behavior summarized above. In agreement with calculations,[18] the 2_1 helix appears to be the energetically preferred conformation for PMEPL and PMPPL and is thus found for samples crystallized at room temperature. Furthermore, the apparent absence of a polymorph analogous to the α-phase of PPL suggests that crystal forms containing right- and left-handed helices are not favored for the optically active polymers considered. This is consistent with the fact that, in such cases, helices of opposite handedness are of different energy. The extended chain, although of higher energy than the 2_1 helix, is accessible at elevated temperatures, and isotactic PMEPL crystallizes from the melt in this conformation. The existence of this polymorph indicates that the higher energy of the planar zigzag conformation is compensated by improvements in crystal packing. Such behavior may be unique to the optically active polymers because of the difficulties associated with the dense packing of helices of a single handedness,[24] which serve to disfavor crystallization in the helical conformation. This packing limitation, however, is not present in the case of the stereocomplex. Each isotactic component can adopt the helical conformation of preferred handedness, resulting in a equimolar mixture of left and right helices.

Unlike PMEPL, isotactic PMPPL crystallizes from the melt, not as an extended chain, but as a 2_1 helix. This can be attributed to the elevation of the relative energy of the planar zigzag conformation of PMPPL by increased steric interference between neighboring side chains.

Acknowledgment. We acknowledge Prof. R. St. John Manley for useful suggestions concerning epitaxial crystallization. This work has been possible through the financial support of the Natural Sciences and Engineering Research Council of Canada and the Department of Education of the Province of Quebec (FCAR program).

References and Notes

(1) Knoblock, F. W.; Statton, W. O. U.S. Patent 3,299,171, 1967.
(2) Prud'homme, R. E.; Marchessault, R. H. *Makromol. Chem.* **1974**, *175*, 2705.
(3) Meille, S. V.; Konishi, T.; Geil, P. H. *Polymer* **1984**, *25*, 773.
(4) Prud'homme, R. E.; Marchessault, R. H. *Macromolecules* **1974**, *7*, 541.
(5) Brückner, S.; Meille, S. V.; Porzio, W. *Polymer* **1988**, *29*, 1586.
(6) Meille, S. V.; Brückner, S.; Lando, J. B. *Polymer* **1989**, *30*, 786.
(7) Marchessault, R. H.; St-Pierre, J.; Duval, M.; Pérez, S. *Macromolecules* **1978**, *11*, 1281.
(8) Cornibert, J.; Marchessault, R. H.; Allegrezza, E. A., Jr.; Lenz, R. W. *Macromolecules* **1973**, *6*, 676.
(9) Duchesne, D.; Prud'homme, R. E. *Polymer* **1979**, *20*, 1199.
(10) Grenier, D.; Prud'homme, R. E.; Leborgne, A.; Spassky, N. *J. Polym. Sci., Polym. Chem. Ed.* **1981**, *19*, 1781.
(11) Lenz, R. W.; d'Hondt, G.; Bigdeli, E. *Polym. Prepr. (Am. Chem. Soc., Div. Polym. Chem.)* **1977**, *18*, 81.
(12) Spassky, N.; Leborgne, A.; Reix, M.; Prud'homme, R. E.; Bigdeli, E.; Lenz, R. W. *Macromolecules* **1978**, *11*, 716.
(13) Ritcey, A. M.; Prud'homme, R. E. *Macromolecules* **1992**, *25*, 972.
(14) Lavallée, C.; Prud'homme, R. E. *Macromolecules* **1989**, *22*, 2438.
(15) Ambeault, Y. M.Sc. Thesis, Université Laval, Sainte-Foy, Québec, Canada, 1991.
(16) Wittmann, J. C.; Lotz, B. *J. Polym. Sci., Polym. Phys. Ed.* **1981**, *19*, 1853.
(17) Wittmann, J. C.; Lotz, B. *J. Polym. Sci., Polym. Phys. Ed.* **1981**, *19*, 1837.
(18) Cornibert, J.; Marchessault, R. H. *Macromolecules* **1975**, *8*, 296.
(19) Perego, G.; Melis, A.; Cesari, M. *Makromol. Chem.* **1972**, *157*, 269.
(20) Cornibert, J.; Hien, N. V.; Brisse, F.; Marchessault, R. H. *Can. J. Chem.* **1974**, *52*, 3742.
(21) Cornibert, J. Doctoral Thesis, University of Montreal, Montreal, Québec, Canada, 1972.
(22) Ferro, D. R.; Brückner, S.; Meille, S. V.; Ragazzi, M. *Macromolecules* **1990**, *23*, 1676.
(23) Spassky, N.; Leborgne, A.; Hull, W. E. *Macromolecules* **1983**, *16*, 608.
(24) Wunderlich, B. *Macromolecular Physics*; Academic: New York, 1973; Vol. 1, p 87.
(25) Grenier, D.; Prud'homme, R. E. *Macromolecules* **1983**, *16*, 302.
(26) Grenier, D.; Prud'homme, R. E. *J. Polym. Sci., Polym. Phys. Ed.* **1984**, *22*, 577.